Multiplierless Approximations of the Near-Hilbert Transform Pair of Wavelet Bases

Adeel Abbas (adeel@jhu.edu)

Abstract— **Recently, there has been a significant interest in the design of iterated filter banks in which wavelet bases form an approximate Hilbert transform pair. In this work, we propose a multiplierless implementation of an orthogonal solution that satisfies Hilbert transform constraints, and meets other desirable properties like high coding gain, reduced computational complexity and sufficient regularity. The filters we use for quantization were proposed by Selesnick [2]. Two solutions are discussed, one using lattice structures (Lattice-2) and the other based on lifting scheme (Lifting-6). Several performance comparisons are presented.**

Index Terms— **Dual-tree complex wavelet transform, lifting scheme, multiplierless, lattice structures.**

I. INTRODUCTION

The wavelet transform has been shown to offer solutions to a wide variety of image and signal processing applications, including compression, denoising, classification, and many others. During the last couple of years, there has been significant progress in the theory and design of M-channel filter banks, and in particular wavelets [15] and [16]. However, there are well known limitations in the conventional wavelet design, for example the lack of directionality, poor shift invariance and lack of phase information. As a result of directional insensitivity, very large number of coefficients is needed to represent smooth contours. With poor shift invariance, it is hard to predict the output with a shift in input. The aim of research in complex wavelet transform is to explore solution to these limitations, on top of the existing nice features that wavelets have to offer.

Several authors have proposed that in a formulation where two dyadic wavelet bases form a Hilbert transform pair, DWT can offer many benefits and provide answer to some of the aforementioned limitations. Shown in Fig. 1, Kinsbury's complex dual-tree DWT [12] and [13] has received considerable interest. In dual-tree, two real wavelet trees are used, each capable of perfect reconstruction. One tree is used to generate the real part of the transform and the other to generate the complex part. It has been shown in [1] that if filters in both trees are offset by half-sample, two orthogonal wavelets form a very close approximation to the Hilbert pair.

Let H_0 and H_1 be a Conjugate Quadrature Mirror (CQF) pair in the real-coefficient branch. Likewise, G_0 and G_1 is another CQF pair. All Filters considered here are orthogonal, real-valued and form a power-complementary pair. The Hilbert condition in [1] implies that if:

$$G_0(\omega) = H_0(\omega) \times e^{-j\theta(\omega)}$$

Then:

$$\underset{g}{\psi}(\omega) \approx \begin{cases} -j\underset{h}{\psi}(\omega) & \omega > 0 \\ j\underset{h}{\psi}(\omega) & \omega < 0 \end{cases}$$

Selesnick in [2] described a systematic design procedure based on spectral factorization. In this procedure, a flat-delay all-pass filter is used to generate half sample delay between $H_0(\omega)$ and $G_0(\omega)$. Using this approach, both orthogonal and biorthogonal (nearly linear-phase) filters with certain regularity and degree of approximation to a half-sample delay were discussed. For orthogonal case, the problem reduces to the design of only two filters: $H_0(\omega)$ and $G_0(\omega)$. The focus of this work is efficient implementation of 12-tap orthogonal filters presented in Example 1A in [2] with 4 vanishing moments and 2rd order all-pass characteristics. The filter coefficients are shown in Table I. For the rest of the paper, we refer to this solution as unquantized filters.

It is well-known that quantizing filter coefficients in FIR direct form does satisfy aliasing cancellation, because filter coefficients get quantized by the same amount. However distortion elimination fails because filters do not remain power-symmetric any more [5]. As a result, perfect reconstruction (PR) can not be achieved. When quantization is done on lattice structures or lifting domain, power-complementary property is preserved and PR is possible. The price paid is in the degree of regularity, because zeros for vanishing moment get perturbed from their actual locations. This introduces DC leakage in the analysis high pass filters and reduces smoothness of scaling functions. Another important consideration is that the output round-off noise contributions in earlier lifting/lattice structures are much severe than later stages [14]. Therefore it is important to reserve more bits for the beginning structures. There has also been interest in designing filters with reduced implementation complexity. Approaches in which coefficients are based on sum of power of two (SOPOT) coefficients are particularly interesting because floating point multiplications can be transformed into simple VLSI-friendly shifts and additions. In [3], an effective design approach is discussed in which a

multiplierless approximation to a transform is found by using coefficients of the form k / 2^n, where the quantization parameter, n indicates the degree of approximation. The factor k is an integer and can be implemented by the minimum adder representation. In general, using more SOPOTs gives closer approximation to unquantized filter coefficients.

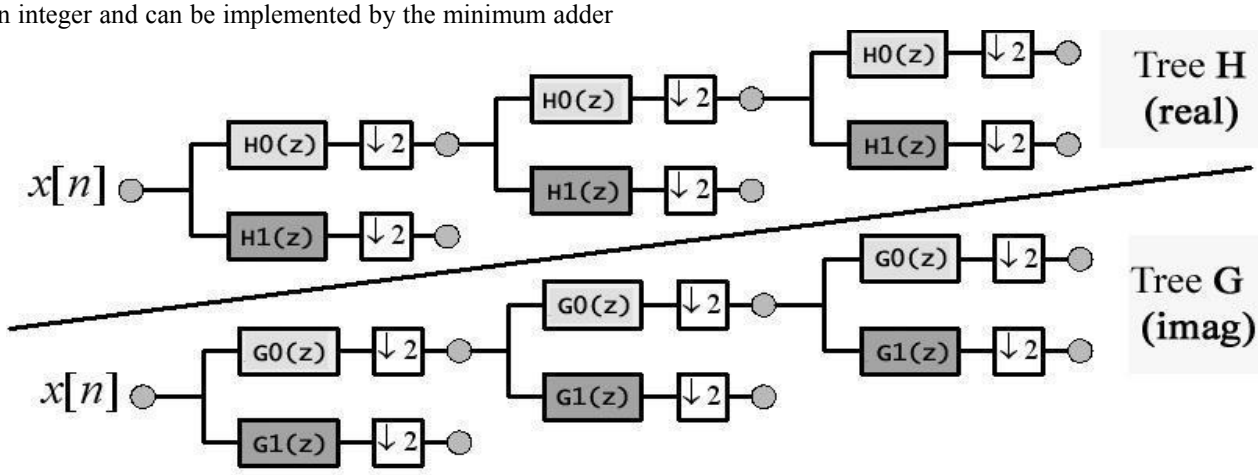

Fig. 1. Kingsbury's complex dual-tree DWT

Table I: Unquantized Filter Coefficients

$h_0(n)$	$g_0(n)$
-0.00178533012604	-0.00035706602521
0.01335887348208	-0.00018475350525
0.03609074349777	0.03259148575321
-0.03472219035063	0.01344990160212
0.04152506151210	-0.05846672525596
0.56035836869367	0.27464307660381
0.77458616704026	0.77956622415107
0.22752075128211	0.54097378940770
-0.16040926912643	-0.04031500786642
-0.06169425120853	-0.13320137936115
0.01709940838890	-0.00591212957013
0.00228522928787	0.01142614643933

Fig. 2 shows zoomed-in view of pole/zero plots of original filters. Both filters have four zeros at z = −1, four complex zeros and three real zeros. The zeros at z = −1.894, z = −0.105, z = −9.472 and z = −0.527 enforce $g_0(n)$ to be a close approximation to half-sample delay of $h_0(n)$. Other zeros are exactly at the same locations.

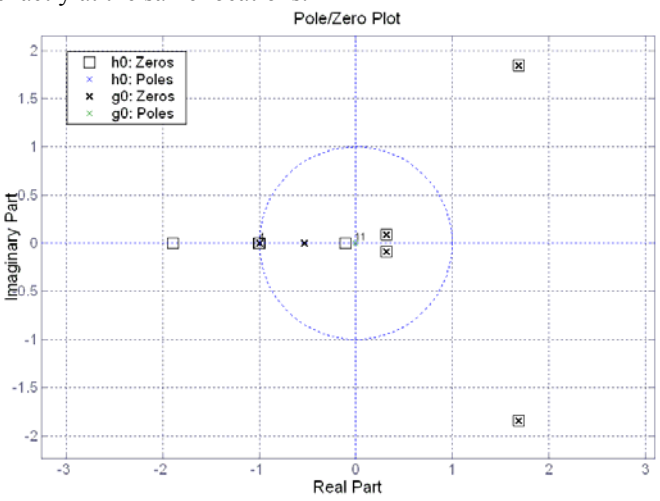

Fig. 2. Pole/Zero plot of $h_0(n)$ and $g_0(n)$

II. QUANTIZED FILTER DESIGNS

We used the software Singular [6] to develop a framework to switch from filter domain to lattice/lifting domain and vice versa. Based on the experiments, a lattice structure in which each coefficient is represented as k / 2^2 represents the best tradeoff in terms of performance and complexity. This is expected because for both filters, coefficients are very close to $k \pm 0.25$. This solution is termed Lattice-2. Table II lists unquantized, lattice-2 quantized coefficients and the MSE/PSNR between the two. The new filter coefficients are shown in Table III.

Table II: Unquantized Lattice Coefficients and their Lattice-2 approximations

	$h_0(n)$ Lattice coefficients		$g_0(n)$ Lattice coefficients	
	Unquantized	Lattice-2	Unquantized	Lattice-2
K0	-1.27999997	-1.25000000	-32.0000000	-24.7500000
K1	3.28926611	3.25000000	-2.48548698	-2.50000000
K2	1.75770926	1.75000000	-3.55918646	-3.50000000
K3	-2.40704036	-2.50000000	-0.25932312	-0.25000000
K4	-2.31345916	-2.25000000	7.54474640	7.50000000
K5	-7.48299980	-7.67187500	0.51739997	0.50000000
MSE	0.00005493		0.0000244	
PSNR	40.3817383		43.952437	

Table III: Lattice-2 Quantized Filter Coefficients

$h_0(n)$ K = 31/17445	$h_0(n)$ Floating-point	$g_0(n)$ K = 28/59275	$g_0(n)$ Floating-point
-1	-0.00177700	-1,	-0.00047200
491/64	0.01363000	-1/2	-0.00023600
5155/256	0.03578000	587/8	0.03463000
-10141/512	-0.03520000	437/16	0.01289000
26097/1024	0.04529000	-4127/32	-0.06087000
2658247/8192	0.57660000	38793/64	0.28610000
14166913/32768	0.76830000	424191/256	0.78210000
1930475/16384	0.20940000	71757/64	0.52920000
-363113/4096	-0.15750000	-2911/32	-0.04294000
-34303/1024	-0.05953000	-2257/8	-0.13320000
2455/256	0.01704000	-99/8	-0.00584100
5/4	0.00222100	99/4	0.01168000

The use of lifting scheme in DWT implementation offers some other advantages. Because of its inherent architecture, lifting allows perfect reconstruction, even if a non-linear transform is used at the decoder. This property is used to design wavelet systems that map integers to integers, a transform called Integer Wavelet Transform (IWT). IWT promises to be a very good replacement for hardware architectures that are particularly good with integers, for example fixed point processors or processors with packed data support.

Every lattice rotation can be expressed as a cascade of three lifting structures [7]. If a lattice has a rotation angle α, we can factorize rotation matrix to get two lifting and a dual lifting step:

$$\begin{bmatrix} \cos\alpha & \sin\alpha \\ -\sin\alpha & \cos\alpha \end{bmatrix} \equiv \begin{bmatrix} 1 & (1-\cos\alpha)/\sin\alpha \\ 0 & 1 \end{bmatrix} \begin{bmatrix} 1 & 0 \\ -\sin\alpha & 1 \end{bmatrix} \begin{bmatrix} 1 & (1-\cos\alpha)/\sin\alpha \\ 0 & 1 \end{bmatrix}$$

Above formula was used to generate lifting coefficients from lattice coefficients. For lifting, it turned out that in order to preserve all desirable wavelet properties; a good choice for quantizated coefficient could be of the form $k / 2^6$. This solution is called Lifting-6. Table IV illustrates lifting coefficients and their lifting-6 approximations. The new filter coefficients are shown in Table V.

Table IV: Unquantized Lifting Coefficients and their Lifting-6 approximations

	$h_0(n)$ lifting coefficients				Lifting-6 coefficients for $g_0(n)$			
	(1 – cos α) / sin α		-sin α		(1 – cos α) / sin α		-sin α	
	Unquantized	Lifting-6	Unquantized	Lifting-6	Unquantized	Lifting-6	Unquantized	Lifting-6
L0	-0.48774627	-0.48437500000	0.78802437	0.781250000000	-0.96923816	-0.9687500000	0.99951208	1.0000000000
L1	0.74117346	0.73779296875	-0.95676142	-0.955566406250	-0.67556694	-0.6718750000	0.92772763	0.9218750000
L2	0.58158741	0.57812500000	-0.86917998	-0.875000000000	-0.75775741	-0.7500000000	0.96272290	0.9687500000
L3	-0.66741723	-0.67187500000	0.92347599	0.921875000000	-0.12755203	-0.1250000000	0.25102008	0.2500000000
L4	-0.65717000	-0.65625000000	0.91791698	0.921875000000	0.87620296	0.8564453125	-0.99133030	-0.9882812500
L5	-0.87525356	-0.87500000000	0.99118852	0.984375000000	0.24337662	0.2500000000	-0.45953404	-0.4531250000
MSE	0.00000228				0.00006235			
PSNR	54.1912490				39.8883484			

Table V: Lifting-6 Quantized Filter Coefficients

$h_0(n)$ K = 18/9551	$h_0(n)$ Floating-point	$g_0(n)$ K = 8/18631	$g_0(n)$ Floating-point
-1	-0.00188500	-1	-0.00042900
4081/568	0.01354000	-483/908	-0.00022820
6157/314	0.03696000	13543/152	0.03822000
-2877/152	-0.03568000	9355/239	0.01679000
10607/485	0.04123000	-8630/63	-0.05877000
6585/22	0.56420000	47305/73	0.27800000
42229/103	0.77280000	119769/67	0.76690000
23431/196	0.22530000	28233/22	0.55050000
-18725/222	-0.15900000	-6215/83	-0.03212000
-14271/430	-0.06256000	-6749/19	-0.15240000
2297/253	0.01711000	-3146/185	-0.00729500
139/110	0.00238200	1023/32	0.01371000

III. Performance Metrics

In this section, we define some of the criteria used in evaluating the performance of our implementation.

A. Coding Gain

Transform coding gain is a very desirable property in designing transforms, especially for compression applications. Coding gain relates to the ability of a sub-band coder to compress most of the signal energy in least number of bands. The biorthogonal coding gain C_g is defined as:

$$C_g \triangleq 10\log_{10} \frac{\sigma_x^2}{\left(\prod_{i=0}^{M-1} \sigma_{xi}^2 \left\|f_i\right\|^2\right)^{1/M}}$$

Where:

M	Number of sub-bands
σ_x^2	Variance of input
σ_{xi}^2	Variance of *i*-th sub-band
$\left\|f_i\right\|^2$	L-2 norm of *i*-th synthesis basis function

The input in this calculation is usually assumed to be a first order Gaussian-Markov process with zero-mean and, unit variance and correlation coefficient 0.95. Results of coding gain are tabulated in Table VII (A).

B. Hilbert Transform Properties

In order for the wavelet bases to have good directional sensitivity, it is important for them to be as close to Hilbert transform approximation as possible. For evaluating how close this approximation is, two quantities are defined:

1) Hilbert energy (HE):

$$HE \triangleq \sqrt{\int_{\omega=-\infty}^{0} \left|\psi_h(\omega) + j\psi_g(\omega)\right|^2}$$

2) Hilbert PSNR (HPSNR):

$$HPSNR \triangleq 10\log_{10} \frac{\max\left(\left|\psi_h(\omega) + j\psi_g(\omega)\right|\right)^2}{\int_{\omega=-\infty}^{0} \left|\psi_h(\omega) + j\psi_g(\omega)\right|^2}$$

Plots of the function $\left|\psi_g(\omega) + j\psi_h(\omega)\right|$ for negative frequencies are shown in Fig. 3. An interesting observation is that Hilbert characteristics of Lattice-2 and Lifting-6 are actually better than the original filters. For instance, the

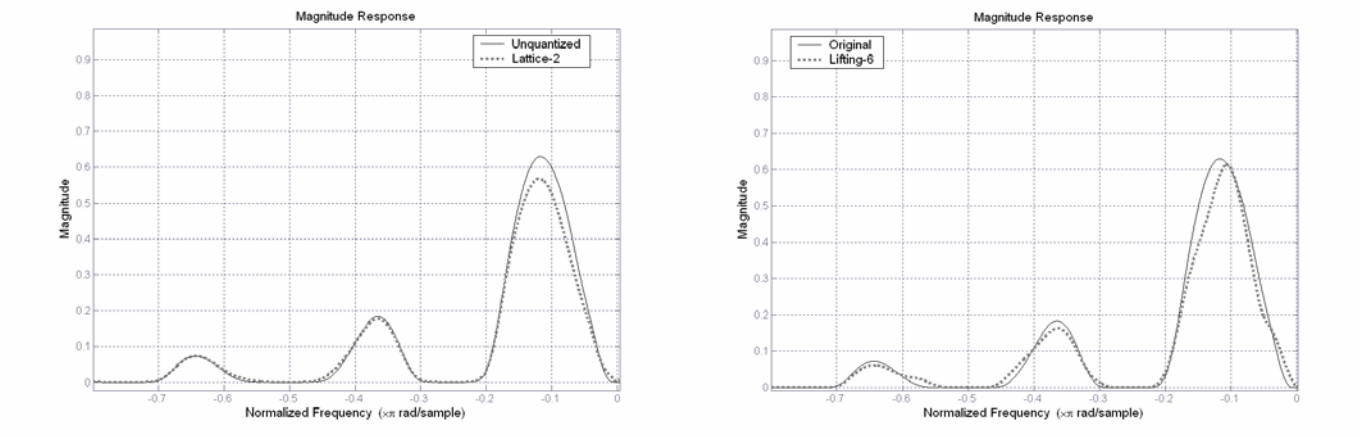

Fig. 3. Approximate Hilbert transform pair of wavelet bases for Lattice-2 (left) and Lifting-6 (right)

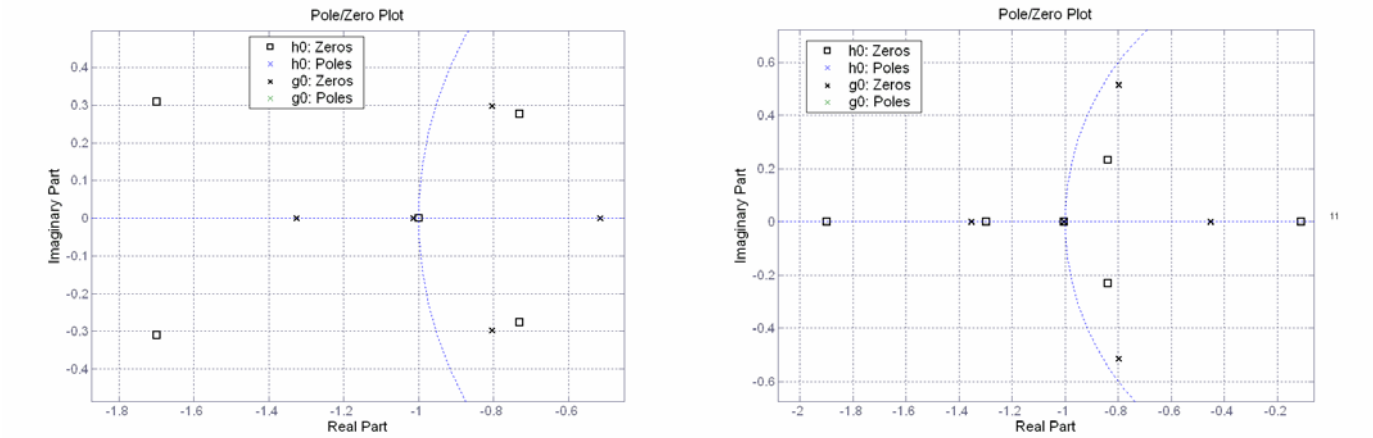

Fig. 4. Zero movement analysis for Lattice-2 (left) and Lifting-6 (right)

Hilbert PSNR of Lattice-2 is 2.28 dB superior to unquantized filters. More insight into this observation will be reported elsewhere. Results are tabulated in Table VII (B, C).

C. *DC Leakage*

Movement of zeros at $Z=-1$ after quantization is also a very important consideration, especially when filters are intended for compression. The DC leakage measures the amount of energy picked up in the high-pass sub-band when a constant signal is presented is an input. Because of DC leakage, the high-pass sub-band is able to capture some energy from polynomials of degree less than $K-1$, K being the regularity. One of the ways to ensure that at least the DC is not captured in the high frequency sub-band is by forcing one zero to be at exactly $z = -1$. This can be achieved by utilizing the fact that sum of all the lattice angles, θ_i must satisfy:

$$\prod_i \theta_i = \{\pi/4, 5\pi/4\} \pm 2\pi k$$

In order to closely approximate above equation, more bits have to be reserved for one of the lattice angles. In Lattice-2 (see Table II), K5 is allotted far more precision bits than other coefficients. Similarly in Lifting-6, L1 needs more resolution to achieve good DC leakage performance. For the moment, the design procedure to find these coefficients is purely heuristic. Pole-Zero plots of filters are shown in Fig. 4. DC leakage PSNR measurements for Lattice-2 and Lifting-6 are shown in Table VII (D).

D. *Smoothness in wavelet and scaling functions*

For reasonable compression performance, the wavelet and scaling functions should be as smooth as possible. Second, they should be as close as possible to the unquantized versions. The selected choices seem to generate functions that are close enough approximations with minimum hardware complexity. In Fig. 5 and 6 wavelet and scaling functions are plotted. For instance, the PSNR for $\psi_h(t)$ between lattice-2 and unquantized was nearly 34.257 dB. Similarly the PSNR for $\Phi_h(t)$ was approximately 37.882 dB. The Sobolev regularity[1], plotted in Table VII (E) is another measure of smoothness of wavelets. Note that the reduced regularity is because quantized filters have only one vanishing moment.

[1]The Sobolev exponents were computed using Matlab code available at: http://www.math.rutgers.edu/~ojanen/

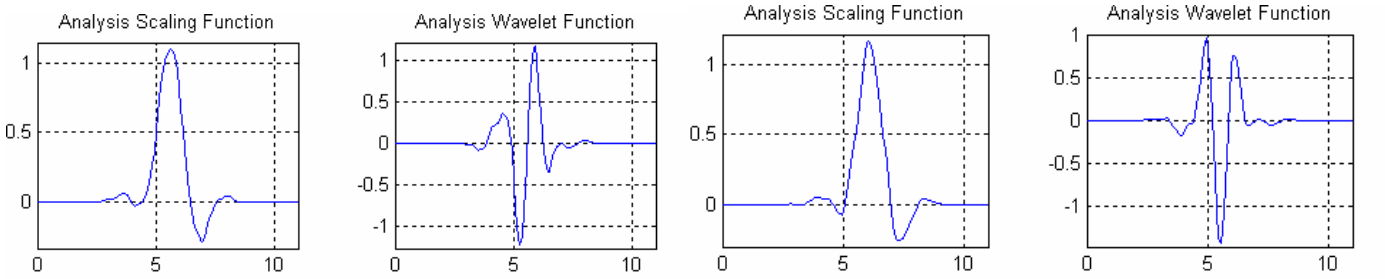

Fig. 5 (a). Lattice-2 Wavelet and Scaling Function for $h_0(n)$ (left) and $g_0(n)$ (right)

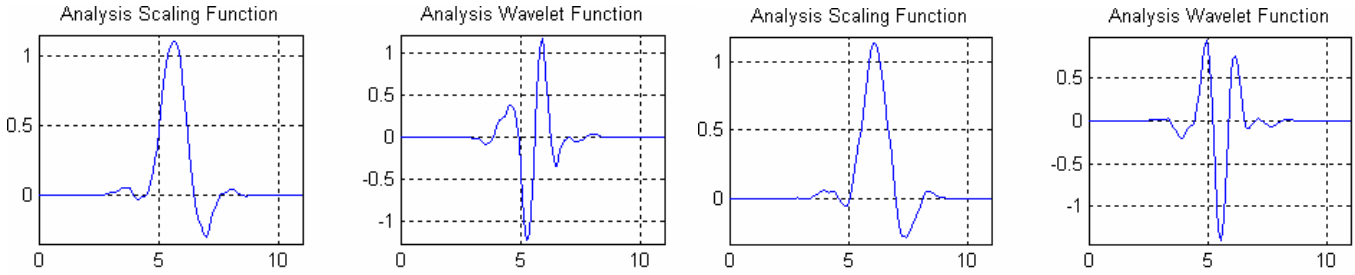

Fig. 6 (a). Lifting-6 Wavelet and Scaling Function for $h_0(n)$ (left) and and $g_0(n)$ (right)

E. Compression performance on benchmark images

Table VI compares compression performance of proposed structures in terms of peak signal to noise ratio (PSNR) and mean square error (MSE) with state of the art Daubechies 9/7 filters and the original filters. The encoder is based on lossy compression with hard thresholding. Only h_0 is considered here because the idea is to use only one of the trees in case compression is the ultimate goal. As evident, the performance is very close to the 9/7 filters and is as good as the original unquantized filters.

F. Directional 2-D Wavelets

A direct consequence of good Hilbert transform pair is better directional selectivity in the 2-D domain. In a traditional 2-D wavelet framework, the directional bases for $\psi_h(x,y)$ are defined as:

$\psi_{h,1}(x,y) \triangleq \phi_h(y)\ \psi_h(x)$	Vertical edges $\theta = 90^o, 270^o$
$\psi_{h,2}(x,y) \triangleq \psi_h(y)\ \phi_h(x)$	Horizontal edges $\theta = 0^o, 180^o$
$\psi_{h,3}(x,y) \triangleq \psi_h(y)\ \psi_h(x)$	Diagonal edges $\theta = 45^o, 135^o, 225^o, 315^o$

The directional bases for $\psi_g(x,y)$ are defined similarly. For the dual-tree, edges at several other angles (15^o, 45^o, 75^o, 105^o, 135^o, 165^o) can be obtained by adding and subtracting $\psi_{h,k}(x,y)$ with $\psi_{g,k}(x,y)$. Further insight into directional 2-D is available in [12]. Fig. 7 plots six 2-D directional wavelets for Lattice-2 design. It is clear that the directional selectivity appears to be very close to the selectivity of unquantized filters.

IV. CONCLUSION

In this paper, two efficient designs of Hilbert transform pair of orthogonal wavelet bases were presented. The computational complexity of Lattice-2 (see Table VIII) requires only 27+24=51 additions per wavelet coefficient pair calculation. In compression applications (for instance in JPEG 2000), h_0 can be used alone. However, when the requirement is to get directionality information, g_0 can be applied to the same data. Afterwards the g_0-coefficients can be combined with h0-coefficients to get a Hilbert transform. Further, all the coefficients are sums of power of two, and as a result the designs can be mapped onto very efficient, multiplierless implementation.

REFERENCES

[1] I. W. Selesnick, "Hilbert transform pairs of wavelet bases," IEEE Signal Processing Letters, vol.8, Iss.6, pp 170-173, Jun 2001.

[2] I. W. Selesnick, "The design of approximate Hilbert transform pairs of wavelet bases, Signal Processing," IEEE Trans. on Signal Processing, vol.50, Iss.5, pp 1144-1152, May 2002.

[3] Y. J. Chen, S. Oraintara, T. D. Tran, K. Amaratunga, and T. Q. Nguyen, "Multiplierless approximation of transforms with adder constraint," IEEE Signal Processing Letters, vol. 9, pp. 344-347, Nov. 2002.

[4] J. Liang and T. D. Tran, "Fast multiplierless approximations of the DCT with the lifting scheme," IEEE Trans. on Signal Processing, vol. 49, pp. 3032-3044, Dec. 2001.

[5] P.P. Vaidyanathan and P.-Q. Hoang, "Lattice structures for optimal design and robust implementation of two-channel perfect-reconstruction QMF banks," IEEE Trans. on Acoustics, Speech, and Signal Processing, Volume 36, pp. 81-94, Jan. 1988.

[6] G. M. Greuel, G. Pfister, H. Schönemann, "Singular Reference Manual Version 2-0-4," Algebraic Geometry Group, Univ. of Kaiserslautern, Germany, http://www.singular.uni-kl.de/, April 2004.

[7] I. Daubechies and W. Sweldens, "Factoring wavelet transform into lifting steps," Tech Rep., Lucent Technologies, Bell Labs, olmodel, NJ, 1996.

[8] A. R. Calderbank, I. Daubechies,W. Sweldens, and B.-L. Yeo, "Wavelet transforms that map integers to integers," Applied and

Computational Harmonic Analysis, vol. 5, no. 3, pp. 332–369, July 1998.

[9] W. Sweldens, "The lifting scheme: A new philosophy in biorthogonal wavelet constructions," in Proc. of SPIE, San Diego, CA, USA, Sept. 1995, vol. 2569, pp. 68–79.

[10] M. J. T. Smith and T. P. Barnwell, III, "A procedure for designing exact reconstruction filter banks for tree structured subband coders," Proc. IEEE ICASSP, Mar. 1984.

[11] W. Sweldens, "The lifting scheme: A custom-design construction of biorthogonal wavelets," Appl. Comput. Harmon. Anal., vol. 3, pp. 186-200, 1996.

[12] N. G. Kingsbury, "The dual-tree complex wavelet transform: a new technique for shift invariance and directional filters," IEEE DSP Workshop 98, Canyon, Aug. 1998.

[13] N. G. Kingsbury, "A dual-tree complex wavelet transform with improved orthogonality and symmetry properties," Proc. IEEE ICIP, Vancouver, Sep. 2000.

[14] B. Zeng and L. Gu, "Roundoff noise analysis of paraunitary filter banks realized in lattice structures," Proc. IEEE Digital signal Processing Workshop, pp. 93-96, Sept. 1996.

[15] P. P. Vaidyanathan, ``Multirate Digital Filters, Filter Banks, Polyphase Networks, and Applications: A Tutorial," Proceesings of the IEEE, Vol. 78 No. 1, pp 56-93, January 1990.

[16] M. Vitterli, "A theory of multirate filter banks," IEEE Trans. On Acoustics, Speech and Signal Processing, vol. 35, pp 356-372, March 1987.

[17] Z. Guangjun, C. Lizhi, and C. Huowang, "A simple 9/7-tap wavelet filter based on lifting scheme," in Proc. IEEE Int'l Conference on Image Processing, vol. 2, 2001, pp. 249–252.

Table VI: Compression performance on standard images

	Ratio	Unquantized		Daub 9/7		Lattice-2				Lifting-6			
						$h_0(n)$		$g_0(n)$		$h_0(n)$		$g_0(n)$	
		MSE	PSNR	MSE	PSNR	MSE	PSNR	MSE	PSNR	MSE	PSNR	MSE	PSNR
Lena	8:1	9.1060	38.1900	7.6003	38.9750	8.8112	38.3330	41.816	31.5699	9.1139	38.1863	47.958	30.9747
	16:1	17.810	35.2765	15.620	35.8463	17.557	35.3388	50.670	30.7358	17.809	35.2768	56.859	30.2353
	32:1	35.300	32.3055	31.976	32.7350	35.117	32.3281	68.533	29.4243	35.300	32.3055	73.909	29.0963
Boat	8:1	13.420	36.2902	12.575	36.5728	13.366	36.3078	22.676	34.0123	13.489	36.2682	24.680	33.6444
	16:1	34.630	32.1733	32.078	32.5058	34.588	32.1787	43.292	31.2038	34.701	32.1644	45.256	31.0112
	32:1	72.110	28.9880	66.438	29.3438	72.082	28.9896	80.076	28.5329	72.150	28.9856	82.171	28.4207
Barbara	8:1	28.443	33.2789	26.234	33.6301	28.243	33.3095	73.647	29.1471	28.351	33.2929	80.768	28.7463
	16:1	75.351	29.0478	72.442	29.2188	75.168	29.0583	121.06	26.9886	75.186	29.0573	126.89	26.7841
	32:1	151.18	26.0235	150.16	26.0532	150.70	26.0375	197.89	24.8545	150.91	26.0314	203.05	24.7425

Table VII: Filter property comparisons of the proposed designs

	A. Coding gain (dB)		B. Hilbert Energy	C. Hilbert PSNR (dB)	D. DC Leakage (dB)		E. Sobolev Exponent	
Filters	$h_0(n)$	$g_0(n)$			$h_0(n)$	$g_0(n)$	$h_0(n)$	$g_0(n)$
Unquantized	9.6229	9.6229	1.30513534	46.6419	279.975	330.606	1.9827	1.9827
Daub 9/7	9.7866	N/A	N/A	N/A	319.091	N/A	1.41 (9)	2.12 (7)
Daub 8/8	9.5794	N/A	N/A	N/A	325.112	N/A	1.7755	N/A
Lattice-2	9.6163	9.6284	1.00186946	48.9220	98.4163	75.2391	0.9971	0.9993
Lifting-6	9.6241	9.6546	1.27918790	46.8476	89.6297	77.4449	0.9998	0.9945

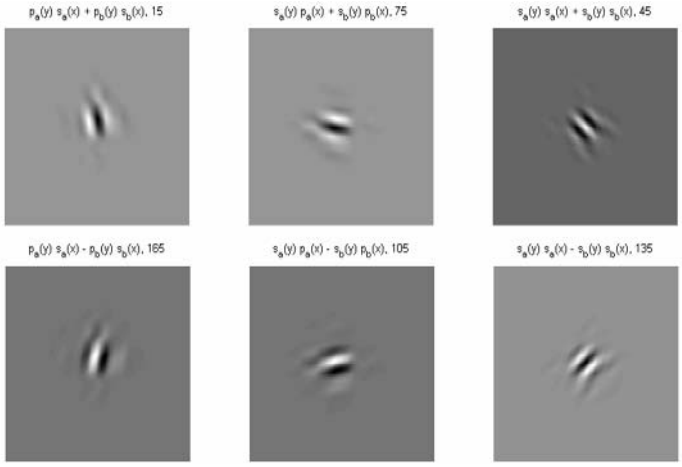

Fig. 7. Directional 2-D Wavelets generated from approximate Hilbert transform pair of Lattice-2 design

Table VIII: Computational complexity of the proposed designs

	Float Mults	Adds	
FIR Direct Form	24	22	
Lattice	12	12	
Lifting	18	18	
Daub 9/7	8	8	
		$h_0(n)$	$g_0(n)$
Lattice-2	0	27	24
Lifting-6	0	65	49